IDENTIFYING METRIC STRUCTURES OF DEEP LATENT VARIABLE MODELS

Stas Syrota, Yevgen Zainchkovskyy
DTU Compute
Technical University of Denmark
{stasy,yeza}@dtu.dk

Johnny Xi & Benjamin Bloem-Reddy
Department of Statistics
University of British Columbia
{johnny.xi,benbr}@stat.ubc.ca

Søren Hauberg
DTU Compute
Technical University of Denmark
sohau@dtu.dk

ABSTRACT

Deep latent variable models learn condensed representations of data that, hopefully, reflect the inner workings of the studied phenomena. Unfortunately, these latent representations are not statistically identifiable, meaning they cannot be uniquely determined. Domain experts, therefore, need to tread carefully when interpreting these. Current solutions limit the lack of identifiability through additional constraints on the latent variable model, e.g. by requiring labeled training data, or by restricting the expressivity of the model. We change the goal: instead of identifying the latent variables, we identify *relationships* between them such as meaningful distances, angles, and volumes. We prove this is feasible under very mild model conditions and without additional labeled data. We empirically demonstrate that our theory results in more reliable latent distances, offering a principled path forward in extracting trustworthy conclusions from deep latent variable models.

1 INTRODUCTION

Latent variable models express the density of observational data through a set of latent, i.e. unobserved, variables that ideally capture the driving mechanisms of the data-generating phenomena. For example, the latent variables of a variational autoencoder (Kingma & Welling, 2013; Rezende et al., 2014) trained on protein data, can reveal the underlying protein evolution which can help domain experts understand a problem of study (Riesselman et al., 2018; Ding et al., 2019; Detlefsen et al., 2022).

Unfortunately, latent variables are rarely identifiable, i.e. they cannot be uniquely estimated from data. This lack of uniqueness prevents reliable analysis of the learned latent variables as the analysis becomes subject to the arbitrariness of model training. Figure 1 exemplifies the issue, where two independently trained latent representations are estimated from transcriptomic data (Tasic et al., 2018). While clusters are similarly estimated across models, the *relationships* between clusters vary significantly, preventing us from extracting intra-cluster information from the plots. This fundamental issue has sparked the development of training heuristics to limit the issue (Kobak & Berens, 2019), and the practice of analyzing latent variables has been both disputed (Chari & Pachter, 2023) and defended (Lause et al., 2024). This entire discussion could have been avoided if only distances between latent variables had been identifiable.

Identifiability guarantees have been heavily investigated. We survey key results in Secs. 2 and 6, but the executive summary is that current approaches require significant model restrictions (e.g. linearity assumptions), labeled data, or a combination of both. These solutions are underwhelming to practitioners who often lack a labeling mechanism and are keen to leverage contemporary generative models.

In this paper, we change the identifiability question to arrive at working tools that do not require data labels and only impose minimal restrictions on the used models. Instead of identifying the latent variables, we identify the *relationship between latent variables*. For example, instead of identifying

the coordinates of the latent variables we identify pairwise distances. In our experience, this matches the needs of domain experts who rarely assign meaning to the coordinates of latent variables. Using differential geometry, we prove strong identifiability guarantees on pairwise distances, angles, and more. We empirically validate our theory on two variational autoencoders.

2 BACKGROUND AND NOTATION

Deep latent variable models learn densities of data $X \in \mathcal{D}$ parametrized by latent variables $Z \in \mathcal{Z}$, such that $p(X) = \int p(X|Z)p(Z)\mathrm{d}Z$ (Tomczak, 2024). We consider models with *continuous* latent variables, i.e., $\mathcal{Z} \subseteq \mathbb{R}^n$. Examples of this model class includes *probabilistic PCA* (Tipping & Bishop, 1999), *variational autoencoders* (Kingma & Welling, 2013; Rezende et al., 2014), *normalizing flows* (Tabak & Vanden-Eijnden, 2010; Lipman et al., 2022), *diffusion models* (Ho et al., 2020) and more.

Formally, a model is a tuple of random variables (Z, X) where the latent Z drives the observations X through a measurable *generator function* $f : \mathcal{Z} \to \mathcal{D}$, often called *the decoder*, and a *noise mechanism* $h : \mathcal{D} \times \mathcal{D} \to \mathcal{D}$ that makes the relationship stochastic through a noise term ϵ,

$$Z_i \sim P_Z, \quad \epsilon_i \sim P_\epsilon, \quad X_i = h(f(Z_i), \epsilon_i)$$

where Z_i's are assumed independent of ϵ_i. We further adopt a standard regularity assumption that h and P_ϵ are such that $\epsilon_a \stackrel{\mathsf{d}}{=} \epsilon_b$, $h(f(Z_a), \epsilon_a) \stackrel{\mathsf{d}}{=} h(f(Z_b), \epsilon_b)$ if and only if $f(Z_a) \stackrel{\mathsf{d}}{=} f(Z_b)$. Here $\stackrel{\mathsf{d}}{=}$ denotes equality in distribution. This assumption ensures that the noise ϵ does not interfere with the causal relationship between X and Z.
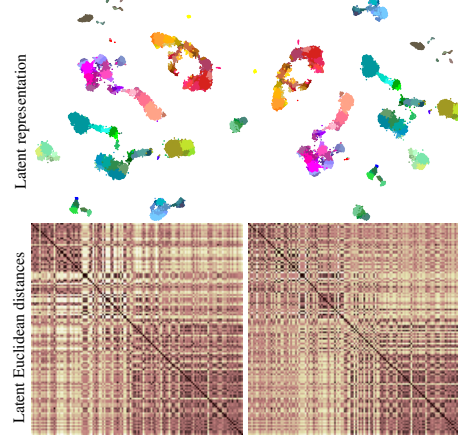

Figure 1: Latent representations of transcriptomic data (top row) changes with model retraining. Each column corresponds to a model trained from scratch. The latent variables are not identifiable and change between training runs. Pairwise Euclidean distances (bottom row, averaged across cell types) also change between runs. This lack of identifiability prevents reliable use of the latent representations to understand the underlying biology.

Statistical model. Given realizations $\mathbf{x}$ of X, learning the generative model means estimating its parameters $\theta = (f, P_Z)$, which represent the decoder and the latent distribution, respectively. These give rise to the marginal distribution of the data P_θ that quantifies model fit. Formally, we define a model M as $M(\mathcal{F}, \mathcal{P}_Z) = \{P_\theta \text{ on } \mathcal{D} \mid \theta = (f, P_Z) \in \mathcal{F} \times \mathcal{P}_Z\}$, where $\mathcal{F}$ and $\mathcal{P}_Z$ are the sets of possible generator functions and distributions on the latent space, respectively. Designing a deep latent variable model means specifying $\mathcal{F}$ and $\mathcal{P}_Z$.

Identifiability concerns the uniqueness of parametrizations. We say that two parameters θ and θ' are equivalent, $\theta \sim \theta'$, if the resulting distributions P_θ and $P_{\theta'}$ are the same. The induced *equivalence class* is denoted $[\theta] = \{\theta' : P_\theta = P_{\theta'}\}$. Informally, this class captures the different ways in which a specific density can be parameterized. Following Xi & Bloem-Reddy (2023), we say that a model is *strongly identifiable* if $[\theta]$ is a singleton, i.e. the model parametrization is unique, while a model is *weakly identifiable* if it can be identified up to the equivalence class $[\theta]$.

For example, probabilistic PCA (Tipping & Bishop, 1999) only identifies the latent variables up to an unknown rotation due to the rotational symmetry of the Gaussian distribution. We then write the equivalence class as $[\theta] = \{R\theta\}$, where R is any rotation matrix (Fig. 2, top).
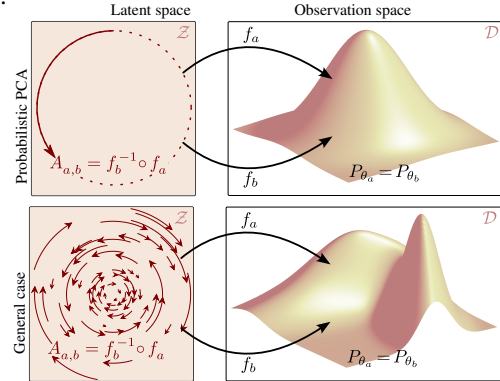

Figure 2: Indeterminacy transformations characterize the identifiability equivalence class. *Top row:* Probabilistic PCA has linear decoders, so the indeterminacy transformations are rotations. *Bottom row:* In general deep latent variable models the indeterminacy transformations are the general class of diffeomorphisms acting on the latent space.

Indeterminacy transformations provides means to characterizing the equivalence class of a latent variable model M (Xi & Bloem-Reddy, 2023). Given two parametrizations of a model $\theta_a = (f_a, P_{Z,a})$ and $\theta_b = (f_b, P_{Z,b})$ with resulting marginal distributions $P_{\theta_a} = P_{\theta_b}$, an *indeterminacy transformation* at (θ_a, θ_b) is a measurable function $A_{a,b} : \mathcal{Z} \to \mathcal{Z}$ such that $P_{\theta_a} = P_{\theta_b}$ and $f_a \circ A_{a,b}^{-1} = f_b$; c.f. bottom panel of Fig. 2. Xi & Bloem-Reddy (2023) prove that the set of all indeterminacy transformations, denoted $\mathbf{A}(M)$, fully determines the equivalence class $[\theta]$. *This result establishes the equivalence between parameter identifiability and indeterminacy transformations of the latent space and their associated decoders.*

Identifiable task capture latent computations with identifiable outcomes (Xi & Bloem-Reddy, 2023). Here, a task is defined by first *selecting* latent points $\mathbf{z}_m = s(\theta, \mathbf{x}_m) \in \mathcal{Z}$, and second evaluating the task $t(\theta, \mathbf{x}_m, s(\theta, \mathbf{x}_m))$. The selection mechanism can e.g. be the inverse decoder, while a task could be independence testing in causal discovery or measuring the distance between latent representations.

Following Proposition 3.1 from Xi & Bloem-Reddy (2023) we can state the sufficient condition for the identifiability of a task in terms of the indeterminacy transformations.

Definition 2.1. A task (s, t) is identifiable at $[\theta]$ if, for each $A \in \mathbf{A}(M)$ with $\mathbf{x}_m \in \mathcal{D}$ and $\mathbf{z}_n \in \mathcal{Z}$:

$$t(\theta, \mathbf{x}_m, \mathbf{z}_n) = t(A\theta, \mathbf{x}_m, A(\mathbf{z}_n)) \quad \text{and} \quad s(A\theta, \mathbf{x}_m) = A(s(\theta, \mathbf{x}_m)), \tag{1}$$

3 PROBLEM STATEMENT

The problem we solve in this paper is to ensure that pairwise distances, and similar quantities, become statistically identifiable in contemporary deep generative models without impractical assumptions. Next, we explicate our assumptions and formalize the goal, which we then solve in Sec. 4.

Following typical literature (Xi & Bloem-Reddy, 2023; Shao et al., 2018), we further impose assumptions on the space of our decoder functions $\mathcal{F}$ and the latent space $\mathcal{Z}$. Our decoders are smooth functions $f : \mathcal{Z} \to \mathcal{D}$ such that for each $f \in \mathcal{F}$:

A1 $\mathcal{Z}$ is compact.

A2 f is injective.

A3 The differential of f has full rank.

A4 All $f \in \mathcal{F}$ have the same image. That is, for any $f_a, f_b \in \mathcal{F}$, we have $f_a(\mathcal{Z}) = f_b(\mathcal{Z}) := \mathcal{M} \subseteq \mathcal{D}$.

Assumptions A2-A4 are repeated from Xi & Bloem-Reddy, whereas we add assumption A1 and require f to be smooth. Together, these allow us to treat the image of the decoder as a smooth manifold. Assumption A1 is purely technical and can be interpreted as (after model training) we consider a compact subset of the latent space, e.g. the range of floating point numbers. Jointly, the assumptions may appear restrictive, but they are satisfied by contemporary models such as $\mathcal{M}$-flows (Brehmer & Cranmer, 2020), normalizing flows, and diffusion models. VAEs need not satisfy A2. On the other hand, A3 can be empirically validated after model training (Shao et al., 2018), and experiments (Sec. 5) show that our methodology is effective in this setting.

In this paper, we shift focus from identifiability of latent representations (or equivalently, model parameters) and instead identify the task of measuring distances in latent space. In particular, we seek to establish a distance measure that is invariant under the indeterminacy transformations $\mathbf{A}(M)$ of a deep latent variable model and therefore identifiable.

Problem 1. Consider a deep latent variable model $M(\mathcal{F}, \mathcal{P}_Z)$ and $\mathbf{A}(M)$ its set of indeterminacy transformations. We want to identify latent distances, i.e. find a 'meaningful' distance function $d : \mathcal{Z} \times \mathcal{Z} \to \mathbb{R}_+$, such that given a parametrization θ and for any $\mathbf{z}_1, \mathbf{z}_2 \in \mathcal{Z}$ and for all $A \in \mathbf{A}(M)$:

$$d(\mathbf{z}_1, \mathbf{z}_2) = d(A(\mathbf{z}_1), A(\mathbf{z}_2)) \tag{2}$$

The inclusion of 'meaningful' in the problem definition emphasizes that solutions can be constructed that satisfy Eq. 2 without being of particular value.

4 MAIN RESULTS

Strategy and results at a glance. In the following, we show that distances, angles, volumes, and more, can be identified in latent variable models that satisfy the weak assumption in the previous

section. Our proof strategy is to connect *indeterminacy transformations* from the identifiability literature with *charts* from the differential geometry literature. Once this connection is in place, our results easily follow. Furthermore, we use the connection to show that identifying Euclidean distances in the latent space is either impossible or requires forcing the decoder to have zero curvature. Below we present results and leave proofs and details to Appendices A and B.

4.1 Identifiability via geometry

We begin by focusing on the family of decoders $\mathcal{F}$ and analyzing the properties of their image.

Lemma 4.1. *Let $\mathcal{Z}$ and $\mathcal{D}$ be two smooth manifolds and $f \in \mathcal{F}$, then f is a smooth embedding and $f(\mathcal{Z}) \subset \mathcal{D}$ is a submanifold in $\mathcal{D}$. In particular, $f : \mathcal{Z} \to f(\mathcal{Z})$ is a diffeomorphism.*

One consequence of Lemma 4.1 is that given two trained models θ_a and θ_b with equivalent marginal distributions $P_{\theta_a} = P_{\theta_b}$, the resulting decoder functions f_a, f_b act as reparametrizations of the same manifold $f_a(\mathcal{Z}) = f_b(\mathcal{Z}) = \mathcal{M}$. In particular the tuples $(f_a^{-1}, \mathcal{M})$ and $(f_b^{-1}, \mathcal{M})$ can be seen as coordinate charts of the manifold $\mathcal{M}$. This situation is the main subject of our analysis and is illustrated in Figure 3. In what follows, we will label the latent spaces by the associated models such that for θ_a we will have $\mathcal{Z}_a$ and similarly for θ_b.

We will go between the different charts (or latent spaces) by using *generator transformations* in Definition 4.2 that push and pull along the respective decoders.

Definition 4.2. Given two model parametrizations $\theta_a = (f_a, P_{Z_a})$ and $\theta_b = (f_b, P_{Z_b})$ with $P_{\theta_a} = P_{\theta_b}$, we define the *generator transformation* $A_{a,b} : \mathcal{Z}_a \to \mathcal{Z}_b$ by $A_{a,b}(\mathbf{z}) = f_b^{-1} \circ f_a(\mathbf{z})$ for $\mathbf{z} \in \mathcal{Z}_a$.

Lemma 2.1 in Xi & Bloem-Reddy (2023) shows that any indeterminacy transformation $A \in \mathbf{A}(M)$ must be almost everywhere equal to the generator transformation. Whereas Xi & Bloem-Reddy focus on proving this result and using it for characterizing identifiability issues in general, we use this construction to show that it preserves the geometric properties of the manifold and, in particular, that the geodesic distance function (formally defined in Def. 4.6) is invariant w.r.t. to the entire set $\mathbf{A}(M)$.

Lemma 4.3. *Given two equivalent parametrizations $\theta_a = (f_a, P_{Z_a})$ and $\theta_b = (f_b, P_{Z_b})$ of a model with $P_{\theta_a} = P_{\theta_b}$, the generator transformations $A_{a,b}(\mathbf{z})$ and $A_{a,b}^{-1}(\mathbf{z}) = A_{b,a}(\mathbf{z})$ are diffeomorphisms.*

From the geometric perspective, if we collect all coordinate charts of the form $(f^{-1}, \mathcal{M})$ stemming from the indeterminacy transformations in $\mathbf{A}(M)$ into a smooth atlas, then Lemma 4.3 tells us that the generator transforms play the of role of smooth transition maps between them (Fig. 3).

Lemma 4.1 tells us that the image of our decoder functions is a smooth manifold. Due to the 'Existence of Riemannian Metrics' result by Lee (2003), it admits a *Riemannian metric g* that for each point p on the manifold defines an inner product in its tangent space at p, denoted by $T_p\mathcal{M}$. The tuple $(\mathcal{M}, g)$ defines the Riemannian manifold structure that allows measurements on general smooth manifolds and is the theoretical foundation for our methodology.

For general data manifolds, there is neither a unique nor a known metric g. However, given a decoder f and a chosen metric (often Euclidean) $g^\mathcal{D}$ in the ambient space $\mathcal{D}$, we can construct the *pullback* metric g^f in the latent space $\mathcal{Z}$ by pulling the ambient metric to the latent space through the decoder.

Definition 4.4. Let $\mathcal{Z}$ be a smooth manifold and $(\mathcal{D}, g^\mathcal{D})$ be a Riemannian manifold. Furthermore, let $f : \mathcal{Z} \to \mathcal{M} \subseteq \mathcal{D}$ be a map satisfying assumptions A1-A3, the pullback metric $f^* g^\mathcal{D}$ on $\mathcal{Z}$ is:

$$(f^* g^\mathcal{D})_p(u, v) = g_{f(p)}^\mathcal{D}(\mathrm{d}f_p(u), \mathrm{d}f_p(v)) \tag{3}$$

for any tangent vectors $u, v \in T_p\mathcal{Z}$. In Eq. 3, $g_{f(p)}^\mathcal{D}$ means that we use ambient metric evaluated in the tangent space $T_{f(p)}\mathcal{M}$. The notation $\mathrm{d}f_p(u)$ means that the differential map of f at $p \in \mathcal{Z}$ maps the vector $u \in T_p\mathcal{Z}$ to $f(u) \in T_{f(p)}\mathcal{M}$. We will denote the pullback metric as $g^f = f^* g^\mathcal{D}$ for shorter notation and let the domain of it be implicit from the definition of f.

The result of this important construction is that: (1) it allows us to construct a Riemannian metric on $\mathcal{M}$ that respect the intrinsic properties of the Riemannian manifold $(\mathcal{M}, g)$. In this setting, the pullback metric g^f represents some intrinsic g in the coordinates defined by $\mathcal{Z}$ and f; (2) we can make all the measurements from the latent space $\mathcal{Z}$ using g^f as this construction makes the Riemannian

manifolds $(\mathcal{Z}, g^f)$ and $(\mathcal{M}, g)$ the same, from a geometric perspective. Thus, we can concentrate our attention on $(\mathcal{Z}, g^f)$, while being consistent with $(\mathcal{M}, g)$ without worrying about g.

The pullback metric merely measures the length of a latent curve by first decoding the curve and measuring its length according to the data space metric. This is a quite 'meaningful' metric in line with the requirements of Problem 1. When the pullback metrics are defined by different decoders that span the same manifold, the generator transformations that comprise the space of indeterminacy transformations are isometries that preserve angles, length of curves, surface areas, and volumes on the manifold.

Figure 3: Decoders f_a and f_b parametrize the same manifold $\mathcal{M} \subset \mathcal{D}$ when $\theta_a = (f_a, P_{Z_a})$ and $\theta_b = (f_b, P_{Z_b})$ give the same marginal distributions $P_{\theta_a} = P_{\theta_b}$. Generator transformation $A_{a.b}$ (Def. 4.2) is the violet path. Pullback metrics assign a local inner product to latent spaces corresponding to measuring *along* the manifold spanned by the decoder. The white ellipsis (left) corresponds to unit circles under the pullback metric, corresponding to a local Euclidean metric in the observation space $\mathcal{D}$. Geodesics (yellow curves) minimize length according to the pullback metric, corresponding to the length of the decoded curve along the manifold.

Theorem 4.5. *Let $\theta_a = (f_a, P_{Z_a})$ and $\theta_b = (f_b, P_{Z_b})$ with $P_{\theta_a}{=}P_{\theta_b}$. Let $(\mathcal{Z}_a, g^{f_a})$ and $(\mathcal{Z}_b, g^{f_b})$ be the associated Riemannian manifolds, then the generator transformation is an isometry making $(\mathcal{Z}_a, g^{f_a})$ and $(\mathcal{Z}_b, g^{f_b})$ isometric. This makes Riemannian geometric properties such as lengths of curves, angles, volumes, areas, Ricci curvature tensor, geodesics, parallel transport, and the exponential map identifiable.*
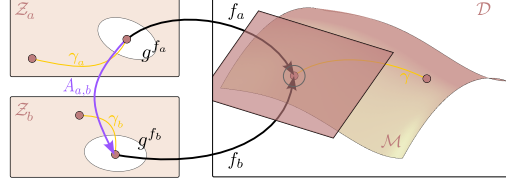
To solve Problem 1, we use the *geodesic distance* and show that it is identifiable in Theorem 4.7.

Definition 4.6. Let $(\mathcal{Z}_a, g^{f_a})$ be a Riemannian manifold. For $\mathbf{z}_1, \mathbf{z}_2 \in \mathcal{Z}$ define the *geodesic distance* as $d_{g^{f_a}}(\mathbf{z}_1, \mathbf{z}_2) = \inf_\gamma \int_a^b |\gamma'(t)|_{g^{f_a}} dt$,where $\gamma : [a, b] \to \mathcal{Z}_a$ is a latent curve from $\mathbf{z}_1$ to $\mathbf{z}_2$.

Figure 3 illustrates how the geodesic distance measures the length of the shortest curve (geodesic), which is equivalent to finding the shortest curve *along* the manifold spanned by a decoder.

Theorem 4.7. *Let $\theta_a = (f_a, P_{Z_a})$ and $\theta_b = (f_b, P_{Z_b})$ with $P_{\theta_a} = P_{\theta_b}$ and let $A_{a,b}$ be the generator transformation between θ_a and θ_b. Furthermore, let $(\mathcal{Z}_a, g^{f_a})$ and $(\mathcal{Z}_b, g^{f_b})$ be the associated Riemannian manifolds. Then, the geodesic distance between $\mathbf{z}_1$ and $\mathbf{z}_2$ is identifiable and for $\mathbf{z}_1, \mathbf{z}_2 \in \mathcal{Z}_a$ we have the following: $d_{g^{f_a}}(\mathbf{z}_1, \mathbf{z}_2) = d_{g^{f_b}}(A_{a,b}(\mathbf{z}_1), A_{a,b}(\mathbf{z}_2))$.*

4.2 IDENTIFIABILITY OF EUCLIDEAN DISTANCES

Theorem 4.7 represents our solution to Problem 1 and came from the geometric take on identifiability. While Sec. 6 outlines alternative approaches to the same problem, in the following we show that these must necessarily impose implicit constraint of flatness on the models.

Proposition 4.8. *Let $\mathcal{Z} = \mathbb{R}^n$ be the latent space and $(\mathcal{Z}, g^f)$ the associated Riemannian manifold. Furthermore, let g^{E_p} denote a metric tensor proportional to the Euclidean metric tensor g^E. Then, $(\mathcal{Z}, g^{E_p})$ is identifiable only if the associated $f \in \mathcal{F}$ parametrizes a flat manifold $\mathcal{M}$. Moreover, if we require Euclidean distances in the latent space to be identifiable, then the previous statement applies, and the associated $f \in \mathcal{F}$ must be such that the generator transforms are isometries of $\mathbb{R}^n$.*

4.3 MAIN TAKEAWAYS

Our results can be summarized as follows: (1) The Riemannian metric space of a deep latent variable model is identifiable (Theorem 4.7), making distance measurements in the latent space identifiable and solving Problem 1. (2) Riemannian geometry properties of the learned manifold, such as distances, angles, and volumes, are identifiable (Theorem 4.5), providing a rich framework for probabilistic data analysis. (3) Using Euclidean distances in the latent space is either non-identifiable or requires imposing flatness constraints on the model (Proposition 4.8). (4) Any task whose identifiability depends on the Riemannian metric is identifiable, provided the manifold's properties allow it.

To exemplify the last point, consider the Fréchet mean that generalizes the well-known mean to manifolds (Pennec, 2006). This is obtained by finding the point with minimal average squared distance to the data, $\mu_{\text{Fréchet}} = \operatorname{argmin}_{\mathbf{z}_1 \in \mathcal{Z}} \sum_{i=1}^{N} d_{g^{f_a}}^2(\mathbf{z}_1, \mathbf{z}_i)$.
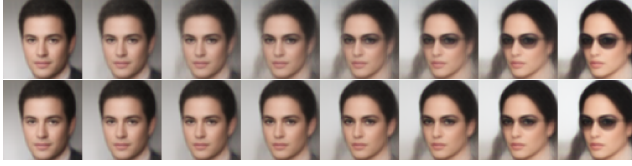
Figure 5: Geodesic (top) and Euclidean (bottom) interpolations, are highly similar, but distances still differ significantly (Fig. 6).

As the mean is defined as an optimization problem, there might exist multiple means, which violates the usual notion of identifiability. First, it is worth noting that the solution set is identifiable, although, in practice, one usually only computes a single optimum. In some situations, this singleton can, however, be identified based on properties of the manifold $\mathcal{M}$. Karcher (1977) and Kendall (1990) provide uniqueness conditions that connect the radius of the smallest geodesic ball containing the data with the maximal curvature of the manifold. Importantly, these are, principally, testable conditions such that it should be feasible to computationally test if a computed mean is identifiable. *Identifiability of some statistical quantities is, thus, within reach.*

5 EXPERIMENTS

By Theorem 4.7, geodesic distances are identifiable while Euclidean ones are not. Consequently, geodesic distances should be more stable under model retraining. To test this hypothesis, we train 30 independent models and compute both Euclidean and geodesic distances between 100 randomly chosen point pairs from the test set. These pairs are the same across all models and we measure the variances of the distances across models.

Figure 4: A latent geodesic from a $\mathcal{M}$-flow model trained on three classes from MNIST. The background color indicates model uncertainty.

To assess the stability of the distance measures, we compute the coefficient of variation for each pair as $\mathrm{CV}(m_{pr}) = \sigma(m_{pr})/\mu(m_{pr})$ with σ and μ denoting standard deviation and the mean, respectively. This is a unitless measure of variability, where low values indicate less variability. We use this to compare the variability of Euclidean and geodesic distances.

We consider two models and datasets. First, a smaller model that satisfies all our assumptions, and second a larger model where we disregard the injectivity assumption. To compute geodesics we parametrize them by a spline connecting two points in the latent space and minimize its energy. The discussion around Definition A.23 in Appendix A covers how this leads to a geodesic. It has been noted that taking decoder uncertainty into account is key to good performance (Arvanitidis et al., 2018; Hauberg, 2018) and we follow the ensemble-based approach from Syrota et al. (2024), implying that we train an ensemble of 8 decoders. Details are in Appendix C and the code to reproduce our results is available at the project GitHub repository.

MNIST with A1-A4 satisfied. We use $\mathcal{M}$-flows (Brehmer & Cranmer, 2020) to construct a VAE with an injective decoder. For visualization, we train on a 3-class subset of MNIST with a 2D latent space. An example geodesic curve from digit 0 to 7 from the test set is shown in Fig. 4. The geodesic crosses class boundaries where they are well-explored by the model and offer little uncertainty.

The left panel of Fig. 6 shows a histogram of CV for the 100 point-pairs, where we see a narrower distribution with both a lower mean and spread for geodesic distances. This demonstrates that identifiability improves reliability.

CELEBA with A2 relaxed and A3 verified. The general VAE model works well due to its flexible neural network decoder with arbitrary architecture that is not guaranteed to be globally injective (A2) nor to have full-rank Jacobian (A3). We train this model on CELEBA Liu et al. (2015) where the architecture is composed of convolutional and dense layers with ELU activation functions. The latent space dimension is 64 and we further employ Resize-Conv layers Odena et al. (2016) to improve image quality. We follow the approach from Shao et al. (2018) to validate that the decoder Jacobian is, indeed, always full rank. An example geodesic is shown in Fig. 5 alongside a Euclidean counterpart, where we do not observe a significant difference between generated images.
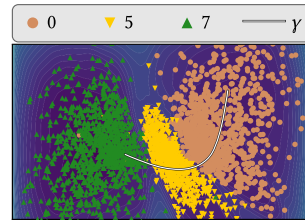
Fig. 6(right) shows that the CV for geodesic distances has both lower mean and standard deviation than Euclidean distances demonstrating that geodesic distances remain more reliable than Euclidean ones even when the injectivity assumption may be violated.

6 RELATIONS TO EXISTING WORK

We connect questions of *identifiability* with results from *differential geometry*. To our knowledge, no previous studies have formally connected these otherwise disjoint fields.

Identifiability is well studied in the ICA or source separation literature (Comon, 1994; Hyvärinen & Pajunen, 1999). The analysis of identifiability in deep generative models stems from a connection between VAEs and ICA first noticed by Khemakhem et al. (2020). Many works either focus on formulating identifiability-enhancing constraints, typically placed on the decoder or latent distribution, or obtaining data from more diverse sources, e.g., multiple environments or multiple views (Kivva et al., 2022; Hyvarinen et al., 2019; Gresele et al., 2019; Locatello et al., 2020; 2019b; Shu et al., 2019). On the other hand, few works exist that characterize when, and what types of non-identifiability are acceptable in deployments of deep generative models without significant constraints.

Latent space geometries have been studied in various contexts to define more 'meaningful' latent interpolations and distances (Tosi et al., 2014; Arvanitidis et al., 2018; Beik-Mohammadi et al., 2021). While Hauberg (2018)
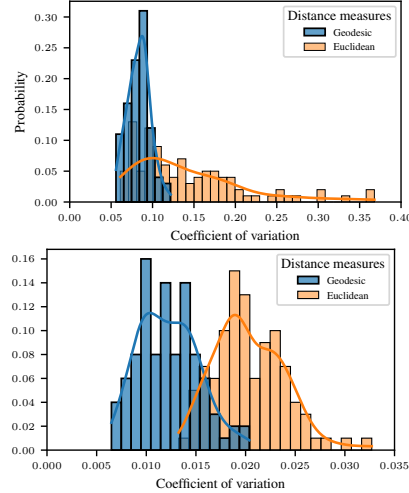

Figure 6: Histograms of coefficients of variation for Euclidean and geodesic distances on MNIST (top) and CELEBA (bottom). Geodesic distances vary less according to one-sided Student's t-test for the null hypothesis that geodesic distances vary less than the Euclidean (p-value of 1.0 and t-statistics -8.64 and -22.33 for MNIST and CELEBA).

alludes to connections between latent space geometries and identifiability, no formal statement has previously been made. Our work, thus, brings further mathematical justification to the algorithmic tools developed for latent space geometries. Detlefsen et al. (2022) has previously demonstrated that latent space geometries recover evolutionary structures from models of proteins that are invisible under an Euclidean latent geometry. Our work adds credibility to these findings.

Causality relies on identifiability as there is little point in recovering the 'true' causal model if it is not unique. The goal of *causal representation learning* (Schölkopf et al., 2021) is closely linked to our quest for identifiable relations between representations. Our approach, however, is not immediately applicable to many questions of causality as these often amount to establishing *independence* between variables (Peters et al., 2017). Under the geometric lens, we do not have a canonical latent coordinate system, which complicates splitting the latent space into independent factors.

Disentanglement can be seen as a 'poor man's causality' (Detlefsen & Hauberg, 2019), where the key generating factors are sought to be axis-aligned in the latent space. This is generally known to be mathematically impossible (Locatello et al., 2019a), much in line with proposition 4.8. Similar to identifiability, this difficulty has been addressed by inductive biases (Bouchacourt et al., 2018) or (weak) data labels (Locatello et al., 2020; 2019b; Shu et al., 2019). Empirical studies, however, hint that some key factors can be recovered in practice (Higgins et al., 2016; Dittadi et al., 2020; Suter et al., 2019). Rolinek et al. (2019) noted that many disentanglement pipelines only work when the variational encoder distribution is restricted to a diagonal covariance, suggesting that current successes may be artifacts of poor Bayesian approximations. Our work suggests that disentanglement is perhaps better achieved by looking for 'geometric factors', such as *principal geodesics* (Fletcher et al., 2004).

Relative representations consider pairwise latent Euclidean distances as a form of representation (Moschella et al., 2022). This is well-aligned with the ideas we put forward. Empirically, Moschella et al. (2022) reports that latent cosine similarities are sufficiently robust to be of practical value, while Yu et al. (2024) empirically investigate geodesic distances.

7 WEAKNESSES AND OPEN QUESTIONS

Our work provides strong identifiability guarantees for essential quantities such as pairwise distances in contemporary generative models. However, our approach does have some pitfalls.

Observation metrics matter. Our identifiable geometric structure relies on the idea of locally bringing the observation space metric into the latent space. This has many benefits but also raises the question of choosing the observation space metric. This choice will directly impact the final latent distances. Did we then replace one difficult problem (identifiability) with another (choosing observation metric)? We argue that most data is equipped with units of measurement, which greatly simplifies the task of picking a suitable metric in the observation space. Furthermore, being explicit about how data is compared improves the transparency of the conducted data analysis. Finally, we emphasize that we are *not* proposing to bring the Euclidean distance from observation space into the latent space, but only to do so *infinitesimally*, i.e. measuring *along* the manifold.

Identifiability comes at a (computational) cost. Euclidean distances are cheap to compute, unlike the geodesic distances we consider. For any geodesic distance, we must solve an iterative optimization problem. Fortunately, this is a locally convex problem, that only requires estimating a limited number of parameters, so the computation is feasible. Yet it remains significantly more costly than computing a Euclidean distance. We argue that when identifiability is important, e.g. in scientific knowledge discovery and hypothesis generation, the additional computational resources are well-spent. Proposition 4.8 effectively tells us that we must choose between (cheap) flat decoders or (expensive) curved ones: we cannot get the best of both worlds.

Compression matters. Our current work rests on the assumption that the latent space has a dimension that is less than or equal to the data space dimension, i.e. $\dim(\mathcal{Z}) \leq \dim(\mathcal{D})$. This remains the standard setting for representation learning and generative models. However, if we, e.g., want to identify distances between the weights of overparametrized neural networks, then our strategies would not directly apply. Early work on understanding the geometric structure of overparametrized models (Roy et al., 2024) suggests that perhaps our approach can be adapted.

Injectivity remains an issue. Most of our assumptions are purely technical and easily satisfied in practice. The key exception is Assumption A2 stating that the decoder f must be *injective*. The decoders of contemporary models such as diffusion models and (continuous) normalizing flows (including those trained with flow matching) are injective and the assumption is satisfied. However, general neural networks cannot be expected to be injective, such that variational autoencoders and similar models are not identifiable 'out of the box'. We have demonstrated that (injective) $\mathcal{M}$-flow architectures can be used for such models, and empirically we observe that the geodesic distance increases robustness in non-injective models. This gives hope that theoretical statements can be made without the injectivity assumption. One such path forward may be to consider notions of *weak injectivity* (Kivva et al., 2022), which is less restrictive and more easily satisfied in practice.

8 CONCLUSION

We have show that latent distances, and similar quantities, can be statistically identified in a large class of generative models that includes contemporary models without imposing unrealistic assumptions. This is a significant improvement over existing work that tends to impose additional restrictions on either model or training data. Our results are significant when seeking to understand the mechanisms that drive the true data-generating process, e.g. in scientific discovery, where reliability is essential.

Practically, it is important to note that our strategy requires no changes to how models are trained. Our constructions are entirely *post hoc*, making them broadly applicable.

Our proof strategy relies on linking identifiability with geometry, which paves a way forward as many tools exist for statistical computations on manifolds. For example, Riemannian counterparts to *averages* (Karcher, 1977), *covariances* (Pennec, 2006), *principal components* (Fletcher et al., 2004), *Kalman filters* (Hauberg et al., 2013), and much more. In principle, it is possible to computationally test if these statistics are identifiable for a given model and dataset. This is, however, future work.

IMPACT STATEMENT

This paper improves our collective understanding of which aspects of a statistical model can be identified. As the theoretical understanding translates directly into algorithmic tools, our work has an impact potential beyond the theoretical questions. Being able to identify relationships between latent representations of data can aid in the process of scientific discovery as we increase the reliability of the data analysis. Our work can also help provide robustness to interpretations of neural networks and other statistical models, which may help in explainability efforts.

REFERENCES

Georgios Arvanitidis, Lars Kai Hansen, and Søren Hauberg. Latent space oddity: on the curvature of deep generative models. In *International Conference on Learning Representations (ICLR)*, 2018.

Hadi Beik-Mohammadi, Søren Hauberg, Georgios Arvanitidis, Gerhard Neumann, and Leonel Rozo. Learning riemannian manifolds for geodesic motion skills. In *Robotics: Science and Systems (RSS)*, 2021.

Diane Bouchacourt, Ryota Tomioka, and Sebastian Nowozin. Multi-level variational autoencoder: Learning disentangled representations from grouped observations. In *Proceedings of the AAAI Conference on Artificial Intelligence*, volume 32, 2018.

Johann Brehmer and Kyle Cranmer. Flows for simultaneous manifold learning and density estimation, 2020.

Tara Chari and Lior Pachter. The specious art of single-cell genomics. *PLOS Computational Biology*, 19(8):e1011288, 2023.

Pierre Comon. Independent component analysis, a new concept? *Signal Processing*, 36(3):287–314, 1994. ISSN 0165-1684. doi: https://doi.org/10.1016/0165-1684(94)90029-9. URL https://www.sciencedirect.com/science/article/pii/0165168494900299. Higher Order Statistics.

Nicki Skafte Detlefsen and Søren Hauberg. Explicit disentanglement of appearance and perspective in generative models. In *Advances in Neural Information Processing Systems (NeurIPS)*, 2019.

Nicki Skafte Detlefsen, Søren Hauberg, and Wouter Boomsma. Learning meaningful representations of protein sequences. *Nature Communications*, 13(1), April 2022. ISSN 2041-1723. doi: 10.1038/s41467-022-29443-w. URL http://dx.doi.org/10.1038/s41467-022-29443-w.

Xinqiang Ding, Zhengting Zou, and Charles L Brooks III. Deciphering protein evolution and fitness landscapes with latent space models. *Nature communications*, 10(1):5644, 2019.

Andrea Dittadi, Frederik Träuble, Francesco Locatello, Manuel Wüthrich, Vaibhav Agrawal, Ole Winther, Stefan Bauer, and Bernhard Schölkopf. On the transfer of disentangled representations in realistic settings. *arXiv preprint arXiv:2010.14407*, 2020.

P Thomas Fletcher, Conglin Lu, Stephen M Pizer, and Sarang Joshi. Principal geodesic analysis for the study of nonlinear statistics of shape. *IEEE transactions on medical imaging*, 23(8):995–1005, 2004.

S.H. Friedberg, A.J. Insel, and L.E. Spence. *Linear Algebra*. Pearson Education, 2014. ISBN 9780321998897. URL `https://books.google.dk/books?id=KyB0DAAAQBAJ`.

Luigi Gresele, Paul K. Rubenstein, Arash Mehrjou, Francesco Locatello, and Bernhard Schölkopf. The incomplete rosetta stone problem: Identifiability results for multi-view nonlinear ica, 2019. URL `https://arxiv.org/abs/1905.06642`.

Søren Hauberg. Only bayes should learn a manifold. 2018.

Søren Hauberg, Francois Lauze, and Kim S. Pedersen. Unscented kalman filtering on riemannian manifolds. *Journal of Mathematical Imaging and Vision*, 46(1):103–120, May 2013.

Søren Hauberg. Differential geometry for generative modeling, 2 2024. URL `https://www2.compute.dtu.dk/~sohau/weekendwithbernie/Differential_geometry_for_generative_modeling.pdf`.

Irina Higgins, Loic Matthey, Arka Pal, Christopher Burgess, Xavier Glorot, Matthew Botvinick, Shakir Mohamed, and Alexander Lerchner. beta-vae: Learning basic visual concepts with a constrained variational framework. 2016.

Jonathan Ho, Ajay Jain, and Pieter Abbeel. Denoising diffusion probabilistic models. *Advances in neural information processing systems*, 33:6840–6851, 2020.

Aapo Hyvarinen, Hiroaki Sasaki, and Richard E. Turner. Nonlinear ica using auxiliary variables and generalized contrastive learning, 2019. URL `https://arxiv.org/abs/1805.08651`.

Aapo Hyvärinen and Petteri Pajunen. Nonlinear independent component analysis: Existence and uniqueness results. *Neural Networks*, 12(3):429–439, 1999. ISSN 0893-6080. doi: https://doi.org/10.1016/S0893-6080(98)00140-3. URL `https://www.sciencedirect.com/science/article/pii/S0893608098001403`.

Hermann Karcher. Riemannian center of mass and mollifier smoothing. *Communications on pure and applied mathematics*, 30(5):509–541, 1977.

Wilfrid S Kendall. Probability, convexity, and harmonic maps with small image i: uniqueness and fine existence. *Proceedings of the London Mathematical Society*, 3(2):371–406, 1990.

Ilyes Khemakhem, Diederik P. Kingma, Ricardo Pio Monti, and Aapo Hyvärinen. Variational autoencoders and nonlinear ica: A unifying framework, 2020. URL `https://arxiv.org/abs/1907.04809`.

Diederik P Kingma and Max Welling. Auto-encoding variational bayes. *arXiv preprint arXiv:1312.6114*, 2013.

Bohdan Kivva, Goutham Rajendran, Pradeep Ravikumar, and Bryon Aragam. Identifiability of deep generative models without auxiliary information, 2022. URL `https://arxiv.org/abs/2206.10044`.

V. Klema and A. Laub. The singular value decomposition: Its computation and some applications. *IEEE Transactions on Automatic Control*, 25(2):164–176, 1980. doi: 10.1109/TAC.1980.1102314.

Dmitry Kobak and Philipp Berens. The art of using t-sne for single-cell transcriptomics. *Nature Communications*, 2019.

R. Kress. *Numerical Analysis*. Graduate Texts in Mathematics. Springer New York, 2012. ISBN 9781461205999. URL `https://books.google.dk/books?id=Jv_ZBwAAQBAJ`.

Jan Lause, Philipp Berens, and Dmitry Kobak. The art of seeing the elephant in the room: 2d embeddings of single-cell data do make sense. *bioRxiv*, 2024.

J.M. Lee. *Introduction to Smooth Manifolds*. Graduate Texts in Mathematics. Springer, 2003. ISBN 9780387954486. URL `https://books.google.dk/books?id=eqfgZtjQceYC`.

Yaron Lipman, Ricky TQ Chen, Heli Ben-Hamu, Maximilian Nickel, and Matt Le. Flow matching for generative modeling. *arXiv preprint arXiv:2210.02747*, 2022.

Ziwei Liu, Ping Luo, Xiaogang Wang, and Xiaoou Tang. Deep learning face attributes in the wild. In *Proceedings of International Conference on Computer Vision (ICCV)*, December 2015.

Francesco Locatello, Stefan Bauer, Mario Lucic, Gunnar Raetsch, Sylvain Gelly, Bernhard Schölkopf, and Olivier Bachem. Challenging common assumptions in the unsupervised learning of disentangled representations. In Kamalika Chaudhuri and Ruslan Salakhutdinov (eds.), *Proceedings of the 36th International Conference on Machine Learning*, volume 97 of *Proceedings of Machine Learning Research*, pp. 4114–4124. PMLR, 09–15 Jun 2019a. URL https://proceedings.mlr.press/v97/locatello19a.html.

Francesco Locatello, Michael Tschannen, Stefan Bauer, Gunnar Rätsch, Bernhard Schölkopf, and Olivier Bachem. Disentangling factors of variation using few labels. *arXiv preprint arXiv:1905.01258*, 2019b.

Francesco Locatello, Ben Poole, Gunnar Raetsch, Bernhard Schölkopf, Olivier Bachem, and Michael Tschannen. Weakly-supervised disentanglement without compromises. In Hal Daumé III and Aarti Singh (eds.), *Proceedings of the 37th International Conference on Machine Learning*, volume 119 of *Proceedings of Machine Learning Research*, pp. 6348–6359. PMLR, 13–18 Jul 2020. URL https://proceedings.mlr.press/v119/locatello20a.html.

Luca Moschella, Valentino Maiorca, Marco Fumero, Antonio Norelli, Francesco Locatello, and Emanuele Rodolà. Relative representations enable zero-shot latent space communication. *arXiv preprint arXiv:2209.15430*, 2022.

Augustus Odena, Vincent Dumoulin, and Chris Olah. Deconvolution and checkerboard artifacts. *Distill*, 2016. doi: 10.23915/distill.00003. URL http://distill.pub/2016/deconv-checkerboard.

B. O'Neill. *Elementary Differential Geometry*. Academic Press, 1997. ISBN 9780125267458. URL https://books.google.dk/books?id=4uMAw3NwnmgC.

Xavier Pennec. Intrinsic statistics on riemannian manifolds: Basic tools for geometric measurements. *Journal of Mathematical Imaging and Vision*, 25:127–154, 2006.

Jonas Peters, Dominik Janzing, and Bernhard Schölkopf. *Elements of causal inference: foundations and learning algorithms*. The MIT Press, 2017.

Danilo Jimenez Rezende, Shakir Mohamed, and Daan Wierstra. Stochastic backpropagation and approximate inference in deep generative models. In *International conference on machine learning*, pp. 1278–1286. PMLR, 2014.

Adam J Riesselman, John B Ingraham, and Debora S Marks. Deep generative models of genetic variation capture the effects of mutations. *Nature methods*, 15(10):816–822, 2018.

Michal Rolinek, Dominik Zietlow, and Georg Martius. Variational autoencoders recover pca directions (by accident). In *Proceedings IEEE Conf. on Computer Vision and Pattern Recognition*, pp. 132, 2019.

Hrittik Roy, Marco Miani, Carl Henrik Ek, Philipp Hennig, Marvin Pförtner, Lukas Tatzel, and Søren Hauberg. Reparameterization invariance in approximate bayesian inference. In *Neural Information Processing Systems (NeurIPS)*, 2024.

I. J. Schoenberg. Contributions to the problem of approximation of equidistant data by analytic functions. part b. on the problem of osculatory interpolation. a second class of analytic approximation formulae. *Quarterly of Applied Mathematics*, 4:112–141, 1946. URL https://api.semanticscholar.org/CorpusID:125667988.

Bernhard Schölkopf, Francesco Locatello, Stefan Bauer, Nan Rosemary Ke, Nal Kalchbrenner, Anirudh Goyal, and Yoshua Bengio. Toward causal representation learning. *Proceedings of the IEEE*, 109(5):612–634, 2021.

Hang Shao, Abhishek Kumar, and P. Thomas Fletcher. The Riemannian Geometry of Deep Generative Models . In *2018 IEEE/CVF Conference on Computer Vision and Pattern Recognition Workshops (CVPRW)*, pp. 428–4288, Los Alamitos, CA, USA, June 2018. IEEE Computer Society. doi: 10.1109/CVPRW.2018.00071. URL `https://doi.ieeecomputersociety.org/10.1109/CVPRW.2018.00071`.

Rui Shu, Yining Chen, Abhishek Kumar, Stefano Ermon, and Ben Poole. Weakly supervised disentanglement with guarantees. *arXiv preprint arXiv:1910.09772*, 2019.

Raphael Suter, Djordje Miladinovic, Bernhard Schölkopf, and Stefan Bauer. Robustly disentangled causal mechanisms: Validating deep representations for interventional robustness. In Kamalika Chaudhuri and Ruslan Salakhutdinov (eds.), *Proceedings of the 36th International Conference on Machine Learning*, volume 97 of *Proceedings of Machine Learning Research*, pp. 6056–6065. PMLR, 09–15 Jun 2019. URL `https://proceedings.mlr.press/v97/suter19a.html`.

Stas Syrota, Pablo Moreno-Muñoz, and Søren Hauberg. Decoder ensembling for learned latent geometries. In Sharvaree Vadgama, Erik Bekkers, Alison Pouplin, Sekou-Oumar Kaba, Robin Walters, Hannah Lawrence, Tegan Emerson, Henry Kvinge, Jakub Tomczak, and Stephanie Jegelka (eds.), *Proceedings of the Geometry-grounded Representation Learning and Generative Modeling Workshop (GRaM)*, volume 251 of *Proceedings of Machine Learning Research*, pp. 277–285. PMLR, 29 Jul 2024. URL `https://proceedings.mlr.press/v251/syrota24a.html`.

Esteban G Tabak and Eric Vanden-Eijnden. Density estimation by dual ascent of the log-likelihood. *Communications in Mathematical Sciences*, 8(1):217–233, 2010.

Bosiljka Tasic, Zizhen Yao, Lucas T Graybuck, Kimberly A Smith, Thuc Nghi Nguyen, Darren Bertagnolli, Jeff Goldy, Emma Garren, Michael N Economo, Sarada Viswanathan, et al. Shared and distinct transcriptomic cell types across neocortical areas. *Nature*, 563(7729):72–78, 2018.

Michael E Tipping and Christopher M Bishop. Probabilistic principal component analysis. *Journal of the Royal Statistical Society Series B: Statistical Methodology*, 61(3):611–622, 1999.

Jakub M Tomczak. Why deep generative modeling? In *Deep Generative Modeling*, pp. 1–13. Springer, 2024.

Alessandra Tosi, Søren Hauberg, Alfredo Vellido, and Neil D. Lawrence. Metrics for probabilistic geometries. In *The Conference on Uncertainty in Artificial Intelligence (UAI)*, Quebec, Canada, July 2014.

Quanhan Xi and Benjamin Bloem-Reddy. Indeterminacy in generative models: Characterization and strong identifiability, 2023.

Hanlin Yu, Berfin Inal, and Marco Fumero. Connecting neural models latent geometries with relative geodesic representations. In *UniReps: 2nd Edition of the Workshop on Unifying Representations in Neural Models*, 2024. URL `https://openreview.net/forum?id=gYTblmieFc`.

A   RIEMANNIAN GEOMETRY

This appendix covers the necessary concepts and results from differential geometry. For more full treatment, the reader is referred to excellent sources such as the book by Lee (2003).

The notation in this appendix is self-contained and separated from the main sections of the paper. Thus, the symbols that were used in the main body can be reused in the following but denote a different concept. The notation is introduced as we go along and should not lead to confusion.

To gradually build up the necessary constructions bottom-up, we start from the concept of a topology that we will morph into a Riemannian manifold by progressively adding structure.

A.1   TOPOLOGICAL CONCEPTS

A topology $\mathcal{T}$ on a set X is a collection of subsets of X, that defines which sets are open in X. This gives rise to the notion of a neighborhood of a point $p \in X$ for an abstract set X.

Definition A.1. A topology $\mathcal{T}$ on X is a collection of subsets of $\mathcal{P}(X)$ satisfying the following axioms:

1. X and $\varnothing$ are in $\mathcal{T}$.

2. The union of any family of subsets in $\mathcal{T}$ are in $\mathcal{T}$.

3. The intersection of any finite family of subsets in $\mathcal{T}$ are in $\mathcal{T}$.

The tuple $(X, \mathcal{T})$ is called a topological space, and the elements of $\mathcal{T}$ are called open sets.

To construct a topology, we need a basis.

Definition A.2. A basis for a topology $\mathcal{T}$ on a set X is a collection $\mathcal{B}$ of subsets of X such that:

1. For each $x \in X$, there is at least one $B \in \mathcal{B}$ such that $x \in B$.

2. If $x \in B_1 \cap B_2$ for $B_1, B_2 \in \mathcal{B}$, then there is a $B_3 \in \mathcal{B}$ such that $x \in B_3 \subseteq B_1 \cap B_2$.

In cases where we work with subsets of X, we can use the topology of X to define a topology on the subsets.

Definition A.3 (Subspace Topology). Let X be a topological space with topology $\mathcal{T}$ and $Y \subseteq X$. The subspace topology on Y is defined as $\mathcal{T}_Y = \{Y \cap U | U \in \mathcal{T}\}$.

The notion of a topological leads to the construction of topological manifold that is the prerequisite to a Riemannian manifold.

Definition A.4. Suppose M is a topological space. We say that M is a topological manifold of dimension n or a topological n-manifold if it has the following properties:

1. M is a Hausdorff space: for every pair of distinct points $p, q \in M$, there are disjoint open subsets $U, V \subseteq M$ such that $p \in U$ and $q \in V$.

2. M is second-countable: there exists a countable basis for the topology of M.

3. M is locally Euclidean of dimension n: each point of M has a neighborhood that is homeomorphic to an open subset of $\mathbb{R}^n$.

Definition A.4 specifies what we mean by a homeomorphism.

Definition A.5. Let X and Y be topological spaces, a map $F : X \to Y$ is

- continuous if the preimage of every open set in Y is open in X.

$$\forall V \subseteq Y \text{ open } \Rightarrow F^{-1}(V) \subseteq X \text{ open}$$

- injective if $F(x) = F(y)$ implies $x = y$.

- surjective if for every $y \in Y$ there is an $x \in X$ such that $F(x) = y$.

- bijective if it is both injective and surjective.

- homeomorphism if it is bijective and both F and F^{-1} are continuous.

If F is a homeomorphism, then X and Y are called homeomorphic. If F, on the other hand, is not bijective but only injective, we call F a topological embedding.

Definition A.6. Let X and Y be topological spaces; a continuous injective map $F : X \to Y$ is called a topological embedding if it is a homeomorphism onto its image $F(X) \subseteq Y$ in the subspace topology.

The notion of local homeomorphism defined in the following is fundamental to the construction of a Riemannian manifold.

Definition A.7. For two topological spaces X and Y, a continuous map $F : X \to Y$ is called a local homeomorphism if every point $p \in X$ has a neighborhood $U \subseteq X$ such that $F(U)$ is open in Y and F restricts to a homeomorphism from U to $F(U)$.

Definition A.4 requires the existence of a local homeomorphism from M to $\mathbb{R}^n$ for every point $p \in M$ defined on a neighborhood U of p. Each such local homeomorphism with the corresponding restriction $U \in M$ is called a coordinate chart.

Definition A.8. A coordinate chart on M is a pair (U, ϕ) where U is an open subset of M and $\phi : U \to \hat{U}$ is a homeomorphism from U to an open subset $\hat{U} = \phi(U) \subseteq \mathbb{R}^n$.

It follows from the definition of a topological manifold M that every point $p \in M$ lies in the domain of some chart. U is called coordinate domain and ϕ local coordinate map. The foundation of a smooth manifold is a maximal smooth atlas containing coordinate charts that are smoothly compatible.

Definition A.9. Let M be a topological n-manifold. Two charts (U, ϕ) and (V, ψ) are called smoothly compatible if $U \cap V = \varnothing$ or their transition map

$$\psi \circ \phi^{-1} : \phi(U \cap V) \to \psi(U \cap V)$$

is a diffeomorphism in case $U \cap V \neq \varnothing$.

In Definition A.9, note how the smoothness of the transition map can be analyzed in terms of the smoothness of maps between open subsets of $\mathbb{R}^n$, namely the domains of the associated coordinate charts.

Definition A.10. A diffeomorphism between two open subsets U and V of $\mathbb{R}^n$ is a bijective map $F : U \to V$ such that both F and F^{-1} are continuous and differentiable.

A.2 SMOOTH MANIFOLDS

We are now in a position to define a smooth manifold.

Definition A.11. Let M be a topological manifold,

- an atlas $\mathcal{A}$ is a collection of charts whose domains cover M

- a smooth atlas is an atlas $\mathcal{A}$ such that any two charts in $\mathcal{A}$ are smoothly compatible

- a maximal smooth atlas is a smooth atlas that is not properly contained in any larger smooth atlas

- M together with a maximal smooth atlas $\mathcal{A}$ is called a smooth manifold denoted by $(M, \mathcal{A})$

In the following, we define smoothness for a map between two smooth manifolds.

Definition A.12. Let M, N be smooth manifolds, and let $F : M \to N$ be any map. We say that F is a smooth map if for every $p \in M$, there exist smooth charts (U, φ) containing p and (V, ψ) containing $F(p)$ such that $F(U) \subseteq V$ and the composite map $\psi \circ F \circ \varphi^{-1}$ is smooth from $\varphi(U)$ to $\psi(V)$. This means that $\psi \circ F \circ \varphi^{-1}$ is a map between subsets of $\mathbb{R}^n$ and $\mathbb{R}^n$ and we can apply the usual real calculus.

Since a manifold does not have the usual operations of the Euclidean vector space, one way to construct a tangent vector space to a manifold M at a point $p \in M$ is to define it in terms of a tangent vector to some curve $\gamma : I \to M$.

Definition A.13. Let M be a smooth manifold, and let $\gamma_1, \gamma_2 : (-\epsilon, \epsilon) \to M$ be smooth curves in M. Suppose that $\gamma_1(0) = \gamma_2(0) = p \in M$, then γ_1 and γ_2 are said to be equivalent if the following holds:

$$\frac{d(\varphi \circ \gamma_1)}{dt}\bigg|_{t=0} = \frac{d(\varphi \circ \gamma_2)}{dt}\bigg|_{t=0}$$

This defines an equivalence relation on the set of all smooth curves through p, and the equivalence classes are called tangent vectors of M at p. The tangent space T_pM to M at p is then defined as the set of all tangent vectors at p and does not depend on the choice of the coordinate chart φ.

A vector space structure on the tangent space T_pM is defined by using the coordinate charts that map between subsets of $\mathbb{R}^n$ and allow us to do vector addition and scalar multiplication. Lee (2003) shows that the resulting construction is independent of the choice of the charts and that T_pM is an n-dimensional real vector space.

Considering maps between manifolds, we want to link the tangent space of one with the tangent space of the other. This is done by defining the differential $\mathrm{d}F$ of F at a point p, which is a linear mapping from one manifold's tangent space to another's.

Definition A.14. Let M and N be smooth manifolds and $F : M \to N$ be a smooth map. For each $p \in M$ we define a map:

$$\mathrm{d}F_p : T_pM \to T_{F(p)}N$$

called the differential of F at p, which is a linear map between the tangent spaces. The following property defines the differential:

$$\mathrm{d}F_p(v) = \frac{d(\varphi \circ \gamma)}{dt}\bigg|_{t=0}$$

where γ is smooth a curve in M through p with $\gamma'(0) = v$ and φ is a coordinate chart around p. This construction is independent of the choice of the chart φ as shown in Lee (2003).

The differential allows us to assess the rank of a map between two manifolds.

Definition A.15. Given two smooth manifolds M and N a map $F : M \to N$ has constant rank r at $p \in M$ if the linear map $dF_p : T_pM \to T_{F(p)}N$ has rank r. F is called a smooth submersion if its differential is surjective at each point (rank $F = \dim N$). It is called a smooth immersion if its differential is injective at each point (rank $F = \dim M$)

To define new submanifolds as images of maps, we need the concept of a smooth embedding.

Definition A.16. Let M and N be smooth manifolds, a smooth embedding of M into N is a smooth immersion $F : M \to N$ that is also a topological embedding, i.e., a homeomorphism onto its image $F(M) \subseteq N$ in the subspace topology.

Theorem A.17 tells us when an injective smooth immersion is also a smooth embedding.

Theorem A.17. *(Proposition 4.22 in Lee (2003)) Let M and N be smooth manifolds, and $F : M \to N$ is an injective smooth immersion. If any of the following holds, then F is a smooth embedding.*

- *F is an open or closed map.*

- *F is a proper map.*

- *M is compact.*

- *M has empty boundary and $\dim M = \dim N$*

Theorem A.18 tells us that images of smooth embeddings are submanifolds with smooth properties.

Theorem A.18. *(Proposition 5.2 in Lee (2003)) Suppose M and N are smooth manifolds and $F : M \to N$ is a smooth embedding. Let $S = F(M)$. With the subspace topology, S is a topological manifold, and it has a unique smooth structure, making it into an embedded submanifold of N with the property that F is a diffeomorphism onto its image.*

A.3 RIEMANNIAN MANIFOLDS

Proposition 13.3 of Lee (2003) proves the existence of a Riemannian metric g in any smooth manifold N, where g is a smooth, symmetric covariant 2-tensor field on M that is positive definite at each point $p \in N$ and defines an inner product in a tangent space T_pN. The tuple (N, g) is called a Riemannian manifold.

Often, in modeling situations, we think of Theorem A.18, that is, we imagine an embedded submanifold $S \subseteq N$ in some ambient space N. In this case, we say that $F : M \to N$ is a parametrization of S. If there is a Riemannian metric g^N on N, there is a way to measure lengths of vectors in a tangent space to a point on S using g^N as it is embedded in this larger vector space that has a metric. We can use this to construct a metric on S by pulling g^N by F.

Definition A.19. For a map $F : M \to F(M) = S \subset N$ between manifolds M and S, and a metric g^N on N, the pullback metric f^*g^N on M is defined as:

$$(F^*g^N)_p(u, v) = g^N_{F(p)}(\mathrm{d}F_p(u), \mathrm{d}F_p(v)) \tag{4}$$

for any tangent vectors $u, v \in T_pM$.

Given two Riemannian manifolds, we can check if they are isometric by using the pullback metric.

Definition A.20. Given Riemannian manifolds (M, g^M) and (N, g^N), a smooth map $F : M \to N$ is called an isometry if F is a diffeomorphism such that:

$$F^*g^N = g^M \tag{5}$$

In which case we say (M, g^M) and (N, g^N) are isometric

A series of results in Lee (2003) Chapters 13,15,16 show that if two manifolds are isometric through a diffeomorphism F, then F preserves lengths of curves, distances, angles, volumes, and other geometric properties between manifolds.

Definition A.21. Given a Riemannian manifold (M, g) we can define the following:

- length or norm of a tangent vector $v \in T_pM$ is defined to be

$$|v|_g = \langle v, v \rangle_g^{1/2} = g_p(v, v)^{1/2}.$$

- angle between two nonzero tangent vectors $v, w \in T_pM$ is the unique $\theta \in [0, \pi]$ satisfying

$$\cos \theta = \frac{\langle v, w \rangle_g}{|v|_g |w|_g}.$$

- tangent vectors $v, w \in T_pM$ are said to be orthogonal if $\langle v, w \rangle_g = 0$. This means either one or both vectors are zero, or the angle between them is $\pi/2$.

- given a smooth curve $\gamma : [a, b] \to M$ we can define the length of γ to be:

$$\mathrm{L}_g(\gamma) = \int_a^b |\gamma'(t)|_g \, dt$$

and the energy of γ to be:

$$\mathrm{E}_g(\gamma) = \frac{1}{2} \int_a^b |\gamma'(t)|_g^2 \, dt$$

Proposition 13.25 of Lee (2003) shows that given a curve $\gamma : [a, b] \to M$ and a reparametrization $u : [c, d] \to [a, b]$ that is a diffeomorphism, the length of the curve $\tilde{\gamma} = \gamma \circ u$, $\mathrm{L}_g(\tilde{\gamma})$ is equal to $\mathrm{L}_g(\gamma)$.

The notion of the length of a curve given in Definition A.21 allows us to consider the Riemannian distance from p to q $(p, q \in M)$ denoted by $d_g(p, q)$ and defined to be the infimum of L_g over all piecewise smooth curve segments from p to q. A shortest curve is not unique since $\mathrm{L}_g(\gamma)$ is reparametrization invariant, and a set of curves is locally minimizing $\mathrm{L}_g(\gamma)$. One useful parametrization is by arc-length s, which ensures that we move along the curve at a constant speed.

Definition A.22 (Arc-length parametrization). A curve $\gamma : [a, b] \to M$ is said to be parametrized by arc-length if the length of the curve between any two points t_1 and t_2 is equal to the difference in the parameter values $t_2 - t_1$. Formally, γ is parametrized by arc-length if:

$$|\gamma'(t)|_g = 1$$

for all $t \in [a, b]$.

Curves γ that are locally minimizing $\mathrm{L}_g(\gamma)$ and are parametrized by arc-length are called geodesics defined in Definition A.23.

Definition A.23. Given a Riemannian manifold (M, g) and $x, y \in M$ with $x \neq y$, a geodesic curve on between x and y on M is formally defined as a curve $\gamma : I \to M$ that locally minimizes the energy functional

$$\mathrm{E}_g(\gamma) = \frac{1}{2} \int_a^b |\gamma'(t)|_g^2 \, dt$$

over all smooth curves $\gamma : [a, b] \to M$ connecting two given points

$\gamma(a) = x$ and $\gamma(b) = y$, where g is the Riemannian metric tensor on M.

As discussed by, e.g., Hauberg (2024) it is a standard result that a minimizer of the energy functional will necessarily be arc-length parametrized and minimize the length functional.

We can consider the Fréchet mean and variance of a set of points on a manifold.

Definition A.24. Let (M, d_g) be a Riemannian metric space and let $\{x_1 \dots x_N\} \in M$ be points on the manifold. For any point $p \in M$, Fréchet variance is defined to be:

$$\Psi(p) = \sum_{i=1}^N d_g^2(p, x_i)$$

Karcher means are the points $m \in M$ that locally minimize Ψ:

$$m = \arg\min_{p \in M} \sum_{i=1}^N d_g^2(p, x_i)$$

If there exists a unique $m \in M$ that globally minimizes Ψ, then it is a Fréchet mean.

B   PROOFS

Theorem B.1. *(Lemma 4.1 in the main text)*

Let $\mathcal{Z}$ and $\mathcal{D}$ be two smooth manifolds and $f \in \mathcal{F}$, then f is a smooth embedding and $f(\mathcal{Z}) \subset \mathcal{D}$ is a submanifold in $\mathcal{D}$. In particular, $f : \mathcal{Z} \to f(\mathcal{Z})$ is a diffeomorphism.

Proof. By Definition A.15 f is a smooth immersion as it is a smooth map of constant rank with injective differential (assumptions A2-A3). Using Theorem A.17 with the fact that $\mathcal{Z}$ is a compact set (assumption A1) gives us that f is a smooth embedding. Finally, Theorem A.18 gives us that $f(\mathcal{Z})$ is a submanifold of $\mathcal{D}$ and f is a diffeomorphism on its image.   □

Theorem B.2. *(Lemma 4.3 in the main text) Let $f_a, f_b \in \mathcal{F}$ and consider the generator transform $A_{a,b} : \mathcal{Z}_a \to \mathcal{Z}_b$ defined by*

$$A_{a,b}(z) = f_b^{-1} \circ f_a(z)$$

Then $A_{a,b}(z)$ and $A_{a,b}^{-1}(z) = A_{b,a}(z) = f_a^{-1} \circ f_b(z)$ are diffeomorphisms.

Proof. The result follows from Theorem B.1 with the fact that $f_a, f_b \in \mathcal{F}$ have the same image due to assumption A4.   □

Theorem B.3. *(Theorem 4.5 in the main text)*

Let $\theta_a = (f_a, P_{Z_a})$ and $\theta_b = (f_b, P_{Z_b})$ with $P_{\theta_a} = P_{\theta_b}$ and let $(\mathcal{Z}_a, g^{f_a})$ and $(\mathcal{Z}_b, g^{f_b})$ be the associated Riemannian manifolds, then the generator transform is an isometry and it holds that:

$$\left(A_{a,b}\right)^* g^{f_b} = g^{f_a} \tag{6}$$

Thus, making $(\mathcal{Z}_a, g^{f_a})$ and $(\mathcal{Z}_b, g^{f_b})$ isometric. This makes Riemannian geometric properties such as lengths of curves, angles, volumes, areas, Ricci curvature tensor, geodesics, parallel transport, and the exponential map identifiable.

Proof. We first show that the generator transform is an isometry. Let us recall that by definition of the pullback we have:

$$g_p^{f_b}(u, v) = g_{f_b(p)}^{\mathcal{D}}(\mathrm{d}f_{b,p}(u), \mathrm{d}f_{b,p}(v))$$

for $u, v \in T_p\mathcal{Z}_b$ and where $\mathrm{d}f_{b,p}(v)$ denotes the differential of the map f_b at a point $p \in \mathcal{Z}_b$ evaluated on the vector $v \in T_p\mathcal{Z}_b$. Using this, we will check Eq. 6 directly:

$$
\begin{aligned}
\left((A_{a,b})^* g^{f_b}\right)_p (y, w) &= g_{f_b \circ f_b^{-1} \circ f_a(p)}^{\mathcal{D}} \left(\mathrm{d}f_{b, f_b^{-1} \circ f_a(p)}(y), \mathrm{d}f_{b, f_b^{-1} \circ f_a(p)}(w)\right) \\
&= g_{f_a(p)}^{\mathcal{D}} \left(\mathrm{d}(f_b \circ f_b^{-1} \circ f_a)_p(y), \mathrm{d}(f_b \circ f_b^{-1} \circ f_a)_p(w)\right) \\
&= g_{f_a(p)}^{\mathcal{D}} \left(\mathrm{d}f_{a,p}(y), \mathrm{d}f_{a,p}(w)\right) \\
&= g^{f_a}
\end{aligned}
\tag{7}
$$

for $y, w \in T_p\mathcal{Z}_a$.

Since we have shown that the generator transform is an isometry, we can conclude that $(\mathcal{Z}_a, g^{f_a})$ and $(\mathcal{Z}_b, g^{f_b})$ are isometric and thus their Riemannian metric properties are identical O'Neill (1997)[Chapters 6 and 7]. To connect to identifiability, we express any of the properties as a task of the form described in Section 2 and use the isometry result above to conclude that the output will be same. We will show an example of this and prove the claim for the goedesic distance function (Theorem 4.7 in the main text) below.   □

Theorem B.4. *(Theorem 4.7 in the main text)*

Let $\theta_a = (f_a, P_{Z_a})$ and $\theta_b = (f_b, P_{Z_b})$ with $P_{\theta_a} = P_{\theta_b}$ and let $A_{a,b}$ be the generator transform between the parameters. Furthermore, let $(\mathcal{Z}_a, g^{f_a})$ and $(\mathcal{Z}_b, g^{f_b})$ be the associated connected Riemannian manifolds. Then, the geodesic distance between $\mathbf{z}_1$ and $\mathbf{z}_2$ is identifiable and it holds that:

$$d_{g^{f_a}}(\mathbf{z}_1, \mathbf{z}_2) = d_{g^{f_b}}(A_{a,b}(\mathbf{z}_1), A_{a,b}(\mathbf{z}_2)) \tag{8}$$

for some $\mathbf{z}_1, \mathbf{z}_2 \in \mathcal{Z}_a$ be two points in the latent space that correspond to some $\mathbf{x}_1, \mathbf{x}_2 \in \mathcal{M}$ on the manifold.

Proof. We need to check Definition 2.1 to show that the task of measuring distances in the latent space is identifiable using the geodesic distance function.

Let $\mathbf{x}_1, \mathbf{x}_2 \in \mathcal{D}$ be the observed data points and consider the inverse of the decoders as our selection function given $\mathbf{x}_1$:

$$\mathbf{z}_1^a = s(\theta_a, \mathbf{x}_1) = f_a^{-1}(\mathbf{x}_1) \text{ and } s(A\theta, \mathbf{x}_1) = s(\theta_b, \mathbf{x}_1) = f_b^{-1}(\mathbf{x}_1) = \mathbf{z}_1^b \tag{9}$$

in a similar way we obtain $\mathbf{z}_2^a$ and $\mathbf{z}_2^b$. Define the task of measuring distances on the manifold as:

$$\begin{aligned}
t(\theta_a, \{\mathbf{x}_1, \mathbf{x}_2\}, \{\mathbf{z}_1^a, \mathbf{z}_2^a\}) &= d_{g^{f_a}}(\mathbf{z}_1^a, \mathbf{z}_2^a) \\
t(\theta_b, \{\mathbf{x}_1, \mathbf{x}_2\}, \{\mathbf{z}_1^b, \mathbf{z}_2^b\}) &= d_{g^{f_b}}(\mathbf{z}_1^b, \mathbf{z}_2^b)
\end{aligned} \tag{10}$$

To check the selection function, take with $A \in \mathbf{A}(M)$ and some $\mathbf{x}_1 \in \mathcal{D}$. Then,

$$\begin{aligned}
\mathbf{z}_1^b = s(\theta_b, \mathbf{x}_1) &= f_b^{-1}(\mathbf{x}_1) \\
&= f_b^{-1} \circ f_a \circ f_a^{-1}(\mathbf{x}_1) \\
&= A_{a,b}(s(\theta_a, \mathbf{x}_1)) \\
&= A(s(\theta_a, \mathbf{x}_1)) \\
&= A_{a,b}(f_a^{-1}(\mathbf{x}_1)) \\
&= A_{a,b}(\mathbf{z}_1^a)
\end{aligned} \tag{11}$$

where we have used that A is almost everywhere equal to the generator transform $A_{a,b}$ due to Xi & Bloem-Reddy.

To check the task function, let us recall that:

$$d_{g^{f_a}}(\mathbf{z}_1^a, \mathbf{z}_2^a) = \inf_{\gamma} \int_a^b |\gamma'(t)|_{g^{f_a}} \, dt \tag{12}$$

where $\gamma : [c, d] \to \mathcal{Z}_a$ is a curve in $\mathcal{Z}_a$ connecting $\mathbf{z}_1^a$ and $\mathbf{z}_2^a$ such that $\gamma(c) = \mathbf{z}_1^a$ and $\gamma(d) = \mathbf{z}_2^a$.

As a geodesic is not unique, multiple curves result in the infimum in Eq. 12. Let γ_a be one solution, then it is by Definition A.23 a geodesic curve. By Theorem 4.5 we have that $(\mathcal{Z}_a, g^{f_a})$ and $(\mathcal{Z}_b, g^{f_b})$ are isometric, which means that $A_{a,b}$ maps geodesics to geodesics O'Neill (1997), then $\gamma_b : [\tilde{c}, \tilde{d}] \to \mathcal{Z}_b$ constructed from γ_a by $A_{a,b}(\gamma_a)$ is a geodesic in $\mathcal{Z}_b$ and thus a solution for $d_{g^{f_b}}(A_{a,b}(\mathbf{z}_1^a), A_{a,b}(\mathbf{z}_2^a)) = d_{g^{f_b}}(\mathbf{z}_1^b, \mathbf{z}_2^b)$. □

Proposition B.5. *Let $\mathcal{Z} = \mathbb{R}^n$ be the latent space and $(\mathcal{Z}, g^f)$ the associated Riemannian manifold. Furthermore, let g^{E_p} denote a metric tensor that is proportional to the Euclidean metric tensor g^E:*

   P1 *If we choose g^{E_p} as our metric in the latent space then $(\mathcal{Z}, g^{E_p})$ is only identifiable if the associated $f \in \mathcal{F}$ parametrize a flat manifold $\mathcal{M}$.*

   P2 *If we choose the Euclidean distance to be identifiable, then P1 applies and the associated $f \in \mathcal{F}$ are such that the generator transforms are isometries of $\mathbb{R}^n$, i.e. translations, rotations, or reflections.*

Proof. Distance measures proportional to the Euclidean distance measure are characterized by the pullback metric g^f being constant everywhere. If g^f is constant everywhere, its directional derivatives vanish and the curvature is zero. The second point follows from Theorem 4.5 and standard linear algebra, e.g. Friedberg et al. (2014). □

C COMPUTING GEODESICS

A geodesic between a and b is defined to be a curve $\gamma(t)$ defined on some interval (usually $[0, 1]$) such that $\gamma(0) = a$ and $\gamma(1) = b$ minimizing the length functional defined in Definition A.21. In our work, we choose to parametrize a geodesic by a cubic spline Schoenberg (1946) and optimize the energy functional defined in Definition A.21 with respect to the free parameters using gradient methods.

C.1 GEDOESIC PARAMETRIZED BY A CUBIC SPLINE

Having settled on a cubic spline as a parametrization of a geodesic, we will now describe the construction of the spline and use it to derive the free parameters of the resulting curve that we can use when minimizing the energy of that curve.

A cubic spline is a piecewise function with pieces that are cubic polynomials. The points where the pieces meet are called the knots, h, and we want to construct a continuous spline with continuous first and second derivatives. Individual components are polynomials, so we only need to constrain their behavior at the knots to satisfy the requirements. Suppose the knots are known, and we are using the splines to interpolate a set of points. In that case, these constraints and boundary constraints will usually give a system of linear equations that can be solved to find the coefficients of the polynomials. In our setting, however, we are using splines to define a path between two points, and the knots are the unknown parameters of the problem, as well as the coefficients of the polynomials. Furthermore, given that $a, b \in \mathbb{R}^n$, we will look to parametrize a geodesic curve $\gamma(t) = (\gamma_1(t), \ldots, \gamma_n(t)) \in \mathbb{R}^n$ and thus we will have n splines, one for each dimension. In the following, we will describe how such a construction works for one dimension and invite the reader to conceptually repeat this for n dimensions.

Following the idea of Hauberg (2024), we will start by connecting two points in the latent space $(a, b \in \mathbb{R})$ by a straight line $l : [0, 1] \to \mathbb{R}$ defined as $l(t) = a + t(b - a)$ and then find a cubic spline that will start and end in 0 to parametrize a deviation from the line. The result will be a curve $\gamma(t) = l(t) + S(t)$ that will connect the two points on the manifold.

The spline $S(t)$ is defined as a piecewise function with n cubic polynomials with coefficients $a_i, b_i, c_i, d_i \in \mathbb{R}$, each defined on an interval $[h_i, h_{i+1}]$ where h_i are the knots with $h_0 = 0$ and $h_n = 1$ set to be the endpoints.

$$S(t) = \begin{cases} S_1(t) & \text{if } t \in [h_0, h_1] \\ S_2(t) & \text{if } t \in [h_1, h_2] \\ \vdots & \vdots \\ S_n(t) & \text{if } t \in [h_{n-1}, h_n] \end{cases} \tag{13}$$

where each $S_i(t)$ is a cubic polynomial:

$$S_i(t) = a_i + b_i(t) + c_i(t)^2 + d_i(t)^3 \quad \text{for } t \in [h_{i-1}, h_i] \tag{14}$$

In the following, let $\xi = (a_1, b_1, c_1, d_1, \ldots, a_n, b_n, c_n, d_n)$ be a vector of all coefficients of the polynomials in our spline and $\xi[i, j]$ be a subvector of ξ containing the coefficients of the i-th and j-th polynomial.

Boundary conditions mean that we need our first polynomial to start in $(0, 0)$ and the last polynomial to end in $(1, 0)$. This gives us two equations:

$$S_1(0) = a_1 = 0 \quad \text{and} \quad S_n(1) = a_n + b_n + d_n + c_n = 0 \tag{15}$$

which we translate into the following matrix equation of the coefficients ξ and a $2 \times 4n$ matrix B:

$$B\xi^T = \begin{bmatrix} 0 \\ 0 \end{bmatrix} \tag{16}$$

where

$$B = \begin{bmatrix} 1 & 0 & 0 & 0 & \ldots & 0 & 0 & 0 & 0 & 0 \\ 0 & 0 & 0 & 0 & \ldots & 0 & 1 & 1 & 1 & 1 \end{bmatrix} \tag{17}$$

The continuity conditions are met when the values at the knots are the same for the two meeting polynomials. This can be expressed as:

$$S_i(h_i) = S_{i+1}(h_i) \Leftrightarrow S_i(h_i) - S_{i+1}(h_i) = 0 \quad \text{for } i = 1, \ldots, n - 1 \tag{18}$$

and for each knot we can write this as a dot product of the coefficients $\xi[i, i + 1]$ and a vector c_i^0:

$$c_i^0 = \begin{bmatrix} 1 & h_i & h_i^2 & h_i^3 & -1 & -h_i & -h_i^2 & -h_i^3 \end{bmatrix} \tag{19}$$

such that the condition at a knot i becomes:

$$c_i^0 \xi[i, i+1]^T = 0 \tag{20}$$

The conditions of first and second derivatives being continuous can be expressed in a similar way.

$$
\begin{aligned}
S_i'(h_i) = S_{i+1}'(h_i) &\Leftrightarrow S_i'(h_i) - S_{i+1}'(h_i) = 0 \quad \text{for } i = 1, \ldots, n-1 \\
S_i''(h_i) = S_{i+1}''(h_i) &\Leftrightarrow S_i''(h_i) - S_{i+1}''(h_i) = 0 \quad \text{for } i = 1, \ldots, n-1
\end{aligned}
\tag{21}
$$

and we can write these conditions as dot products of the coefficients $\xi[i, i+1]$ and vectors c_i^1 and c_i^2:

$$c_i^1 = \begin{bmatrix} 0 & 1 & 2h_i & 3h_i^2 & 0 & -1 & -2h_i & -3h_i^2 \end{bmatrix} \tag{22}$$

$$c_i^2 = \begin{bmatrix} 0 & 0 & 2 & 6h_i & 0 & 0 & -2 & -6h_i \end{bmatrix} \tag{23}$$

such that the conditions at a knot i become:

$$
\begin{aligned}
c_i^1 \xi[i, i+1]^T &= 0 \\
c_i^2 \xi[i, i+1]^T &= 0
\end{aligned}
\tag{24}
$$

Having defined the smoothness constraints for a given knot i we can construct matrices C^0, C^1, C^2 each with dimensions $(n-1) \times 4n$ where each row i corresponds to the respective constraint at the knot i with $4 \cdot (i-1)$ zeros before the constraint and $4 \cdot (n-1-i)$ zeros after the constraint. E.g. for $n = 4$ the C^0 matrix would look as follows:

$$
C^0 = \begin{bmatrix}
c_1^0 & 0 & 0 & 0 & 0 & 0 & 0 & 0 & 0 \\
0 & 0 & 0 & 0 & c_2^0 & 0 & 0 & 0 & 0 \\
0 & 0 & 0 & 0 & 0 & 0 & 0 & 0 & c_3^0
\end{bmatrix}
$$

where each c_i^0 is a row vector as defined in Eq. 19.

Now, the final system of equations can be written as:

$$
\underbrace{\begin{bmatrix} B \\ C^0 \\ C^1 \\ C^2 \end{bmatrix}}_{:=A} \xi^T = \mathbf{0}
\tag{25}
$$

resulting in $4n - 2$ equations for $4n$ unknowns. To solve this system of equations in an interpolation setting, we usually impose two additional constraints to get a square system of equations. These constraints can be that the second derivative is zero at the endpoints or that the second derivatives at the first and last knots are equal. The former is known in the literature as a natural spline and the latter as not-a-knot spline Kress (2012).

Getting back to our original task of finding free parameters of the curve that we can optimize its energy with respect to, we note that given that we have $4n$ coefficients, the actual number of free parameters is considerably smaller due to the constraints. The problem in Eq. 25 is known as the problem of finding the Null Space of the row space of matrix A. A basis for such null space, denoted by $\mathcal{N}(A)$, can be found by computing the Singular Value Decomposition (SVD) Klema & Laub (1980) of A. If A is of rank r, then SVD of A is given by $A = U\Sigma V^T$ where U and V are orthogonal matrices with dimensions $((4n-2) \times 4n)$ each and Σ is a $(4n \times 4n)$ diagonal matrix with r nonzero singular values in the diagonal. The null space of A is then given by the columns of V^T corresponding to the zero singular values. Treating $\mathcal{N}(A) =: N$ as a $(4n \times (n-r))$ matrix, we have arrived at a set of $n - r$ free parameters ω that we can optimize with respect to. To recover the full set of coefficients ξ, we can use the following equation:

$$\xi = N\omega \tag{26}$$

and evaluate the spline at the desired points to get the curve $\gamma(t)$.

C.2 OPTIMIZING THE SPLINE TO FIND A GEODESIC

In the previous subsection, we have reduced the infinite set of functions in which we are looking for a geodesic to another but considerably smaller, infinite set of splines. The next step is to use optimization to find the spline that minimizes the energy defined in Definition A.21. Calculating the energy requires computing an integral, which is, in practice, approximated by a sum over a discretized interval.

In the following treatment we assume that $\mathcal{D} = \mathbb{R}^n$ and let $f_\theta : \mathcal{Z} \to \mathbb{R}^n$ be a decoder parametrized by θ and $\gamma : [0, 1] \to \mathcal{Z}$ be a spline in the latent space, then the approximation of the energy of γ is given by:

$$
\begin{aligned}
E(\gamma) &= \frac{1}{2} \int_0^1 |\gamma'(t)|_g^2 dt \\
&= \frac{1}{2} \int_0^1 |\frac{\partial}{\partial t} f_\theta(\gamma(t))|_E^2 dt \\
&\approx \frac{1}{2\Delta t} \sum_{i=2}^{n_t} \|f_\theta(\gamma(\bar{t}_i)) - f_\theta(\gamma(\bar{t}_{i-1}))\|^2 =: \bar{E}(\gamma)
\end{aligned}
\tag{27}
$$

where $\{\bar{t}_i\}_{i=0}^{n_t}$ is a sequence of n_t points in the interval $[0, 1]$. Combining this with the discussion in the previous section, we can now define the optimization problem as simply:

$$
\min_{\boldsymbol{\omega}} \quad \bar{E}(\gamma_{\boldsymbol{\omega}})
\tag{28}
$$

where we use $\boldsymbol{\omega} = \{\omega_j\}_{j=1}^k$ to de note the parameters of the k different splines given the dimensionality of the latent space $\mathcal{Z} \in \mathbb{R}^k$ and remind the reader that $\gamma_{\boldsymbol{\omega}}(t) = (\gamma_{\omega_1}^1(t), \dots, \gamma_{\omega_k}^k(t)) \in \mathcal{Z}$.

Using optimization to learn the manifold will result in different approximations depending on the initialization of the parameters and the optimization algorithm used. Considering the problem in light of the first line of Eq. 27, we can see that the Riemannian metric becomes the stochastic term. In this sense, the manifold is stochastic, and the resulting distances between points will be affected by this stochasticity.

Following (Syrota et al., 2024), having access to an ensemble of decoders allows us, in principle, to make the optimization problem in Eq. 28 aware of the uncertainty involved. The methodology effectively uses Monte Carlo methods to compute the energy with respect to the uncorrelated posterior over parameters. This posterior approximated by an ensemble. The following equation is the optimization problem we solve and makes the idea explicit:

$$
\min_{\boldsymbol{\omega}} \quad \frac{1}{2\Delta t} \sum_{i=2}^{n_t} \left\| f_{\hat{\theta}_j}(\gamma_{\boldsymbol{\omega}}(\bar{t}_i)) - f_{\hat{\theta}_k}(\gamma_{\boldsymbol{\omega}}(\bar{t}_{i-1})) \right\|^2
\tag{29}
$$

where $\Delta_t = \bar{t}_i - \bar{t}_{i-1}$ is the step size in the discretization of the interval $[0, 1]$ and is assumed to be constant. The decoders $f_{\hat{\theta}_k}$ and $f_{\hat{\theta}_{kj}}$ are sampled uniformely and independently from the ensemble.